

Dust Removal Experiments for ITER Blanket Remote Handling System

Kenichi UENO, Atsushi ABURADANI, Makiko SAITO, Takahito MARUYAMA,
Nobukazu TAKEDA, Shin MURAKAMI and Satoshi KAKUDATE

Japan Atomic Energy Agency, 801-1 Mukoyama, Naka 311-0193, Japan

(Received 25 September 2013 / Accepted 21 November 2013)

To reduce maintenance workers' dose rate caused by activated dust adhering to the ITER blanket remote handling system (BRHS), dust must be removed from BRHS surfaces. Dust that adheres to the top surface of the BRHS rail from cyclic loading of the vehicle manipulator is considered to be the most difficult dust to remove. Dust removal experiments were conducted to simulate the materials, conditions, and cyclic loading of actual BRHS operations. The tungsten powder used to simulate the dust was squashed, and the area of contact by cyclic load was increased, but the powder was not embedded into the matrix. The increase in the area of contact increased the total intermolecular force between a tungsten particle and the surface, which was considered the main force adhering dust to the test piece surface. A combination of dust removal methods, including vacuum cleaning and brushing, was applied to the simulated dust that adhered to the test pieces. The results showed that vacuum cleaning is effective in removing dust from the non-cyclic loaded surface. The combined methods were highly efficient in removing the dust that strongly adhered to the rail surface.

© 2014 The Japan Society of Plasma Science and Nuclear Fusion Research

Keywords: ITER, blanket remote handling system, activated dust, dust removal method

DOI: 10.1585/pfr.9.1405012

1. Introduction

The ITER blanket remote handling system (BRHS) removes and replaces the blanket modules inside the vacuum vessel (VV) during maintenance operations. The BRHS consists of one or two vehicle manipulators (VMs), an articulated rail, rail support equipment, and cable handling equipment (Fig. 1) [1].

During plasma operations of ITER, the dust produced inside the VV, caused by the interactions between the plasma and surrounding materials, is activated by neutrons during the fusion reaction. The dominant source of activated dust for the dose rate is the product of tungsten activation [2,3]. Following plasma operations, the BRHS is installed into the VV and then performs maintenance operations, which include handling contaminated components in the VV. Therefore, the BRHS is contaminated by the activated dust that accumulates inside the VV. A maintenance operation for the BRHS is performed in the ITER Hot Cell Facility's refurbishment area. However, the BRHS contamination levels must be reduced prior to this hands-on maintenance operation to reduce the workers' dose rate. This study proposes methods for decontaminating BRHS surfaces.

2. Dust Specifications

In ITER, activated dust accumulates inside the VV because of the interactions between the plasma and plasma-

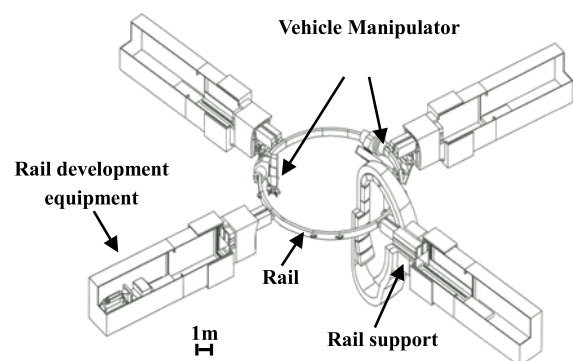


Fig. 1 Schematic view of ITER BRHS with rail deployed 360° with two VMs.

facing components. Tungsten is the dominant dust component during the transformation of deuterium to tritium. The activity and density of dust are estimated from the administrative limits in the ITER preliminary safety report [2]. Dust size is estimated from an existing experimental fusion machine with a count median diameter of 1.32 - 14.39 μm [4, 5].

The most conservative scenario obtained from the safety limit assumption is as follows. All nuclides adhere to the equipment and VV surfaces in the form of dust. In total, 30 kg of dust remains after the cleaning of the VV. Therefore, the density of dust is assumed to be $2.9 \times 10^{-5} \text{ g/mm}^2$ in this study.

author's e-mail: ueno.kenichi@jaea.go.jp

3. Design

The BRHS's smooth round shape and surface finish, along with dust guards for covering the complex parts, enables dust to be easily removed from its surface. However, the top surface of the rail cannot be covered. Therefore, dust adheres to the rail by cyclic loading of the VM and is considered the most difficult part to clean during dust removal.

Consequently, methods for removing this dust are required. Liquid cleaning materials must be avoided for removing this dust, because they would increase the amount of tritium-contaminated liquid waste. In addition, dry-ice-pellet injection for contaminated surfaces must also be avoided, because it causes adverse effects on the hot cell ventilation system. A cleaning method with a vacuum cleaner and plastic wire brush is simple and has no significant adverse effects on waste or the hot cell environment; therefore, we adopted it in this study.

4. Experiment

Testing for simulated dust adhesion to the rail and an assessment of decontamination methods were performed using a mock-up of the rail, rollers, and simulated dust (Allied-material D100 tungsten powder, with an average particle size of 10 μm). Tungsten powder was distributed on the test piece surfaces.

The test pieces were 30 mm in diameter and 20 mm in thickness; they were composed of high-tensile-strength steel HT590. This material simulated the rail material in the BRHS design (SM570).

The surface conditions were simulated with a hard 20- μm chrome-plated surface with a surface roughness (maximum height) of 6.3 μs and a hardness of 774 HV. These conditions were the same as those of the BRHS rail surface design. A pressurized plate was used to simulate the VM roller material (S45C) and the surface conditions of roughness 3.2 μs and hardness 101 HV.

Cyclic loading conditions between the rail and VM were simulated, as shown in Table 1. The number of repetitions was equivalent to the number of passes by the VM in the maintenance plan. The loads were applied to the test pieces covered with tungsten powder using a hy-

draulic servo-controlled fatigue-strength testing machine (Shimadzu Servo Pulsar with a maximum dynamic load rating of 750 kN).

After cyclic loading, the test piece surfaces were observed using a scanning electron microscope (Hitachi S-3600 at an acceleration voltage of 5.00 kV). The test pieces were observed again after the first 60 s of vacuum cleaning and once more after the second 60 s of brushing and vacuuming. Vacuuming was conducted using a CONDOR CVC-105 vacuum cleaner (air flow 3 m^3/min , ultimate vacuum 19.6 kPa, and suction power 980 W) with a nozzle with an inside diameter of 35 mm. To investigate the cyclic-load effect, a non-cyclic-loaded test piece was prepared.

5. Results and Discussion

Figure 2 shows the test piece surface after cyclic loading and 60 s of vacuum cleaning. Residual tungsten particles were observed on the cyclic-loaded part.

Scanning electron microscopy (SEM) images of the test piece surfaces are shown in Fig. 3. Small amounts of tungsten particles remained after the first 60 s of vacuum cleaning in the non-cyclic-loaded sample; however, the dust that adhered by cyclic loading was observed at the center area of the sample. After the additional 60 s of brushing and vacuuming, trace amounts of tungsten particles remained on the surface of both samples.

Following cyclic loading, there were two types of dust distribution: (1) densely packed and (2) dispersed. Enlarged SEM observations following cyclic loading of the sample are shown in Fig. 4. For the densely packed type, tungsten particles were squashed and clumped together, as shown in Fig. 4 (a). For the dispersed type (Fig. 4 (b)), the tungsten particles were squashed but were not embedded into the test pieces.

The increase in the area of contact caused an increase in the total intermolecular force between a tungsten particle and the test piece surface. This intermolecular force was considered the main force for dust adhesion. In addition, increased surface roughness increased the area of contact between a tungsten particle and the test piece surface. To remove the tungsten particles from the surface, a removal force greater than the intermolecular force is

Table 1 Cyclic Loading Conditions.

Compressive force	
Maximum test load	32.62 kN
Minimum test load	1 kN
Maximum Hertzian contact stress (Maximum surface pressure)	795 MPa
Number of repetitions	1000
1 repetition period	5 s
Loaded wave form	sin wave form



Fig. 2 Test piece surface after cyclic loading and 60 s of vacuum cleaning.

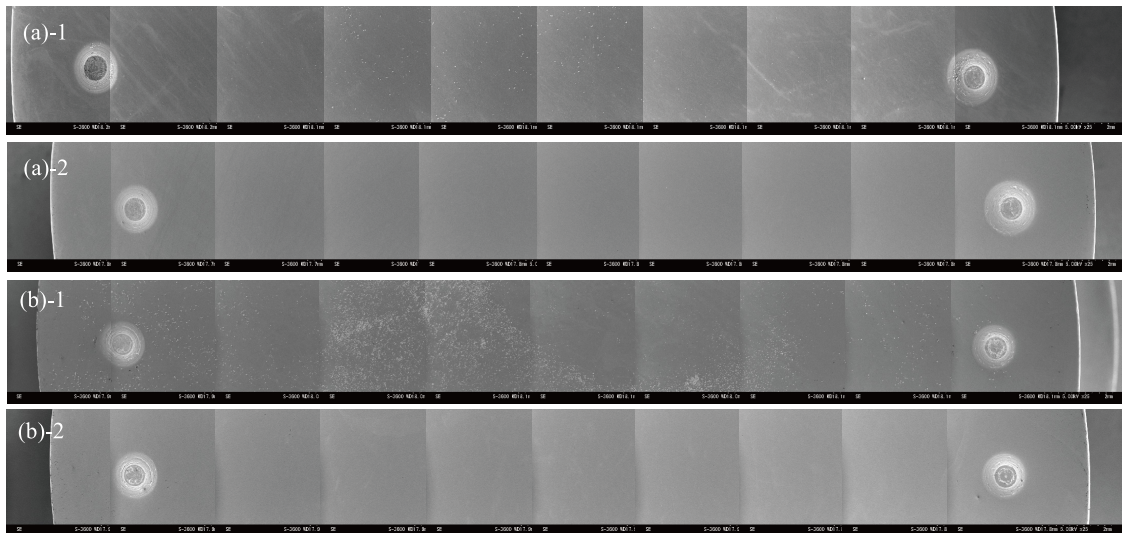


Fig. 3 SEM images of (a) no-cyclic load sample and (b) for cyclic load sample, “-1” for first 60-second vacuum and “-2” for after additional 60-second brushing and vacuum cleaning of each samples.

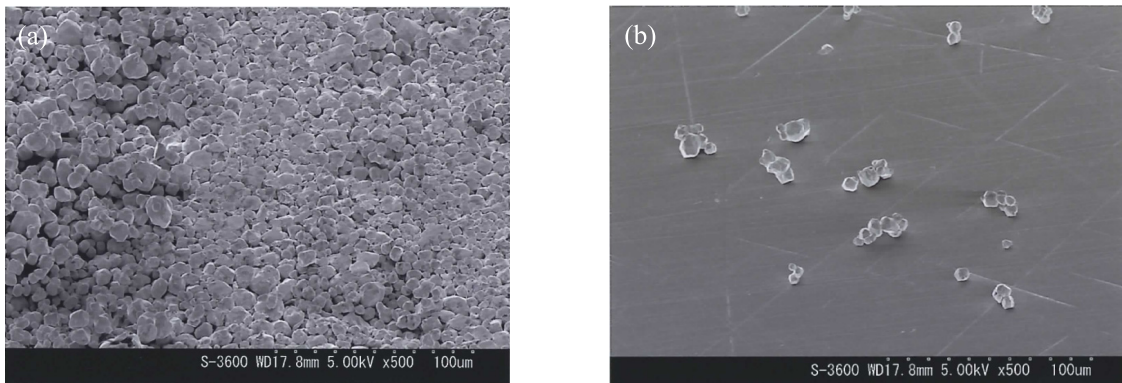


Fig. 4 Enlarged SEM images of parts where particles are (a) densely packed and (b) dispersed.

Table 2 Results of remaining dust calculations for $1.1 \times 10^2 \text{ mm}^2$ (6.7×10^6 pixels).

Load condition	Cleaning method	Area [pixels]	Area [mm^2]	Density [g/mm^2]
No-cyclic load	60-second vacuum cleaning	7.4×10^3	1.2×10^{-1}	2.1×10^{-7}
	Additional 60-second brushing and vacuuming	5.4×10^1	8.6×10^{-4}	1.6×10^{-9}
Cyclic loaded	60-second vacuum cleaning	8.5×10^5	1.4×10^1	2.5×10^{-5}
	Additional 60-second brushing and vacuuming	2.7×10^1	4.3×10^{-4}	7.8×10^{-10}

required. The combination of the 60s of brushing and vacuuming methods was effective in removing the adhered tungsten particles from the surface.

From the SEM images, the number of particles was counted using image processing. Dust-density calculations were conducted for images of the test piece parts’ surfaces that underwent cyclic loading. A total test piece surface area of $1.1 \times 10^2 \text{ mm}^2$ was used for these calculations.

From the brightness intensity information, the SEM

images were then changed to binary images, and the remaining dust weight was calculated from the number of counted particles. A tungsten particle thickness of $10 \mu\text{m}$ and a tungsten density of $19.25 \text{ g}/\text{cm}^3$ were used in the calculations.

The results of density calculations for the remaining dust are summarized in Table 2. Dust reduction rates from the ITER VV dust-density assumption ($2.9 \times 10^{-5} \text{ g}/\text{mm}^2$) were calculated as 7.4×10^{-3} for the first 60s of vacuum

cleaning and 5.4×10^{-5} for the additional 60 s of brushing and vacuuming for the non-cyclic load sample. The dust reduction rate for the cyclic load sample was 8.4×10^{-1} for the first 60 s of vacuum cleaning and 2.7×10^{-5} for the additional 60 s brushing and vacuuming.

Vacuum cleaning was effective in removing dust from the non-cyclic loaded surface. However, it was difficult to remove dust from the cyclic loaded surface; the same order of dust density in ITER VV remained after vacuum cleaning.

Although the 60 s brushing and vacuuming methods were effective in removing dust, trace amounts (10^{-9} g/mm² order) of dust still remained on the test piece surface. This trace amount of dust caused a dose rate on the order of 10^{-9} Sv/h for workers assuming a homogenous planar source.

Although these dust reduction rates seem small for the additional brushing and vacuuming methods, they are strongly affected by the initial value of the calculation. The ITER VV dust density (2.9×10^{-5} g/mm²) was used for the initial value in this calculation, but this value is based on the most conservative scenario. Hence, the calculated dust reduction rates in this study are most likely overestimated; thus, the density of remaining dust (on the order of 10^{-9} g/mm²) must be considered to estimate the workers' dose rate during maintenance.

6. Conclusion

To reduce the maintenance workers' dose rate caused by residual dust on the BRHS surface, dust removal experiments were conducted to simulate the materials, conditions, and cyclic loading of actual BRHS operations. Tungsten powder was used to simulate the dust, and brushing and vacuuming dust removal methods were applied. Dust that adhered to the rail surfaces by cyclic loading of the VM was the most difficult to remove.

Tungsten powder was squashed by cyclic loading but was not embedded into the matrix. The increase in the area of contact caused the increase in the total intermolecular force between a tungsten particle and the surface, which

was considered the main force for dust adhesion. In addition, surface roughness increased the area of contact, which consequently increased the adhesion force.

Vacuum cleaning was effective in the removal of particles from a non-cyclic loaded surface. However, it was difficult to remove dust from the cyclic loaded surface. To remove the tungsten particles from the surface, a removal force greater than the intermolecular force is required. The combination of the 60 s brushing and vacuuming methods was effective in removing the tungsten particles adhered by the cyclic load.

These results showed that for surfaces where the vacuum cleaner and brushing nozzles could reach, dust could be removed. However, it was difficult to remove dust from the complex areas where the vacuum cleaner nozzles could not reach. The BRHS will be designed with the possibility of reducing these complex areas and adding dust protection covers.

Moreover, surface roughness is an important factor for dust adherence. The entire outer surface must be smooth for dust removal. To reduce the workers' dose rate in accordance with the As Low As Reasonably Achievable (ALARA) policy, other dust removal methods must be combined to remove the remaining residual dust.

Acknowledgments

The authors express their deep appreciation to Hitachi High-Technologies Corporation for the SEM observations for this study. The authors thank Mr. N. Duncan for the English language review. The authors would also like to thank Enago (www.enago.jp) for the English language review.

- [1] A. Tesini and J. Palmer, *Fusion Eng. Des.* **83**, 810 (2008).
- [2] Preliminary Safety Report (RPrS) for ITER.
- [3] N.P. Taylor and W. Raskob, *Fusion Sci. Technol.* **52**, 359 (2007).
- [4] J.P. Sharpe *et al.*, *J. Nucl. Mater.* **337–339**, 1000 (2005).
- [5] J.P. Sharpe *et al.*, *J. Nucl. Mater.* **313–316**, 455 (2003).